

RF-Prism: Versatile RFID-based Sensing through Phase Disentangling

Songzhen Yang, Meng Jin, Yuan He and Yunhao Liu

School of Software & BNRist, Tsinghua University

ysz18@mails.tsinghua.edu.cn, mengj@mail.tsinghua.edu.cn, heyuan@tsinghua.edu.cn, yunhao@greenorbs.com

Abstract—The signal phase is one of the most important metrics in RFID-based sensing, which is a useful technique enabling many significant applications. However, existing approaches of RFID-based sensing are often restricted in terms of the sensing capability or accuracy, due to the phase entanglement problem: the phase of the RFID signal is jointly affected by multiple factors, and the change in the signal phase cannot be directly attributed to any one of them. In order to tackle this problem, we propose RF-Prism, a versatile sensing approach that can simultaneously infer multiple physical factors (i.e., location, orientation, and material of targets), purely based on the phase readings. RF-Prism includes a comprehensive model to describe how different physical factors affect the phase of the received signal, and a complete design to disentangle the phase in the multi-frequency and multi-antenna scenario. We implement RF-Prism and evaluate its performance with extensive experiments. The results show that RF-Prism simultaneously achieves a mean localization error of 7.61 cm , a mean orientation error of 9.83 degrees, and 87.9% material identification accuracy, which outperforms state-of-the-art approaches.

Index Terms—RFID, Sensing, Phase

I. INTRODUCTION

Passive Radio-Frequency Identification (RFID), as a major enabler of automatic battery-free identification, has been extensively deployed in various applications [1] [2] [3] [4] [5] [6]. Beyond the traditional identification functions of RFID systems, recent works focus more on its sensing capability. Since the signal received from an RFID tag is affected by the state of the tag and the surrounding environment that the signal propagates through, exploiting the signal metrics like phase and RSSI makes it possible to sense a wide variety of physical factors. For instances, we have witnessed numerous RFID-based sensing applications in object tracking [7] [8], motion recognition [9] [10] [11], material identification [12] [13] [14], vibration sensing [15] [16], localization [17] [18] [19] [20] [21], orientation sensing [22] [23] [24], humidity sensing [25] [26], etc.

In spite of the progress in this area, we find an important fact that is often overlooked: the metric of the RFID signal (typically the phase) is *jointly* affected by all the factors mentioned above, from the location and the orientation of the tag-attached target to the humidity of the environment. In a practical application scenario, the impacts of multiple factors essentially entangle with each other in the phase of the received signal. Consequently, when a change in the signal phase is detected, it is hard to directly attribute this change to any one or a portion of those factors. Neglecting this problem

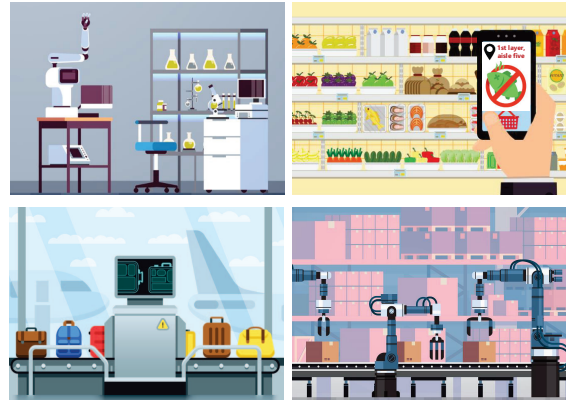


Fig. 1. Application scenarios of RF-Prism.

leads to restricted functions or poor accuracy of RFID-based sensing.

Fig. 1 shows several typical application scenarios of RFID-based sensing, such as the inventory management in chemical labs and hospitals, commodity monitoring in supermarkets, security checking, and automatic production lines. There are many other similar scenarios that have similar challenges on RFID-based sensing. Let's take the inventory management in chemical labs as an example. Every bottle and flask, where chemical is contained, is attached with an RFID tag. Due to the constant taking in and out operations, different chemicals may be placed at the same position on the shelf. The same chemical may also be placed at different positions at different time. Since the location of the bottle and the contained chemical jointly affect the tag's signal, none of the existing sensing system can answer questions like where is a certain chemical or what is the chemical at a specified position.

Looking into the above problem, we find that it is a common limitation of the existing works on RFID-based sensing. The root cause is the entangled impact of different factors on the signal phase. Due to this reason, the existing RFID based localization approaches usually have to assume static RF environment and fixed/known tag orientation [17], while the RFID based material sensing approaches usually need to calibrate for the unknown tag location and orientation [13]. Such designs are compromised against the phase entanglement problem, and are by nature incapable of effective sensing in real-world applications.

This paper presents RF-Prism, a versatile RFID-based sensing approach which is able to directly disentangle the phase reading and infer all the impacting factors simultaneously. Indeed, the phase entanglement problem is essentially an undetermined problem where the known conditions (i.e., phase reading) is not sufficient to solve all the unknown factors. RF-Prism solves this problem by fully exploiting the channel hopping capability of COTS RFID readers and the multi-antenna deployment in most RFID systems. This provides an opportunity to increase the dimensions of known conditions by jointly exploiting information from more dimensions (i.e., multi-frequency and multi-antenna). With the increased amount of conditions, we build a phase-disentangled sensing model where all the factors that contribute to the phase change can be resolved in one-shot phase readings.

RF-Prism's ability of phase disentangling not only improves the accuracy in the estimation of one certain factor but also enables simultaneously estimation of multiple factors, expanding the sensing capability. This extends the application scope of RFID-based sensing, making it able to support advanced and complex applications where multiple factors of one target are simultaneously interested, e.g., the chemical management example mentioned previously.

The contributions of this paper are summarized as follows:

- Based on an in-depth understanding of signal's propagation in the environment, we build a comprehensive model to describe how different physical factors affect the phase of the received signal, and further extend this model to the multi-frequency and multi-antenna scenario.
- We propose the design of RF-Prism and demonstrate a complete workflow of versatile sensing - achieving simultaneously phase-based localization and material sensing.
- We implement RF-Prism on a COTS RFID platform, and evaluate its performance with extensive experiments. Our results show that RF-Prism simultaneously achieve a mean localization error of 7.61cm , a mean orientation error of 9.83° , and 87.9% material identification accuracy, which outperforms state-of-the-art approaches.

The rest of this paper is organized as follows: We review the related works in Section II. Section III presents the design overview. The technique details of signal disentangling and versatile sensing are respectively elaborated in Section IV and Section V. Section VI presents the implementation details and the evaluation results. We conclude this paper in Section VII.

II. RELATED WORKS

In this section, we briefly review the related literatures in RFID phase-based sensing.

Since the phase reading reflects the propagation distance of a tag's signal, by observing the phase changes we can track the location of the tag, realizing applications like localization [17] [19], tracking [8] [7], behavior identification [9] [10], rotation sensing [24] [22], vibration inspection [15] [27], and etc. For example, *BackPos* [18] proposes a hyperbola-based algorithm to determine the position of the target tag using multiple antennas with known geometric structure. It can achieve a

mean accuracy of 12.8cm without using anchor tags. *Tagoram* [7] builds a differential augmented hologram to estimate the probabilities of the tag's existence on the 2D surveillance plane. *Tagbeat* [27] infers the target's vibration frequency by observing the change of the phase reading that caused by the periodical change in the reader-tag distance.

Besides the propagation distance, phase reading is also related to the impedance of tag antenna. Specifically, when attached to or close to targets with different materials, tag's antenna will suffer different amounts of impedance changes. This further leads to different phase changes. Given this phenomenon, we can treat tag as a low-cost material sensor to perform tasks like material identification [12], touch sensing [28], and leakage detection [29] [30]. For example, *Tagtag* [12] demonstrates that phase and RSSI can be used as an indicator to distinguish even genuine and fake perfumes. *TwinLeak* [29] show that it is possible to detect a 10ml liquid leakage on tag with a 97.2% accuracy by simply observing the phase and RSSI change of tag's signal. *RIO* [28] shows that finger touch can also change the impedance of tag antenna, based on which one can use tag array as a low-cost keyboard/tablet to track user's finger movement.

One problem endemic to phased-based RFID localization and sensing is that the phase value is jointly determined by multiple physical factors. So it is indeed difficult to attribute a change in phase to any one or a portion of the factors, making it infeasible to sense any one of the factors. Existing methods address this problem in two ways: i) considering some of the factors as noise and eliminating their impact using signal filtering methods or using special tag deployment; or ii) trying to infer multiple factors simultaneously based on sophisticated signal features which are designed dedicate to estimate particular factors. For example, in detecting liquid leakage, *TwinLeak* [29] uses a dual-tag model to eliminate the impact of tag mobility/human on phase reading. *3D-OmniTrack* [24] propose a polarization-sensitive phase model which can provide both the location and orientation of tags simultaneously in 3D space. *TagRay* [14] uses the change pattern and change range of the phase reading to respectively infer the moving trajectory and material of the target.

However, all of those solutions do not fundamentally solve the phase entanglement problem. They are compromised against the phase entanglement problem and might perform well in the particular scenarios they dedicate to, but suffer poor generality when used in other scenarios. Different from those methods, RF-Prism firstly presents a comprehensive model to directly disentangle the phase by leveraging the frequency and spatial diversities, and then address the entanglement problem for different RFID sensing applications. RF-Prism extends the application scopes of RFID-based sensing, making it able to support advanced and complex functions. Besides, the disentangled signals, in which the ambiguity has been removed, can also improve the performance of existing sensing approaches.

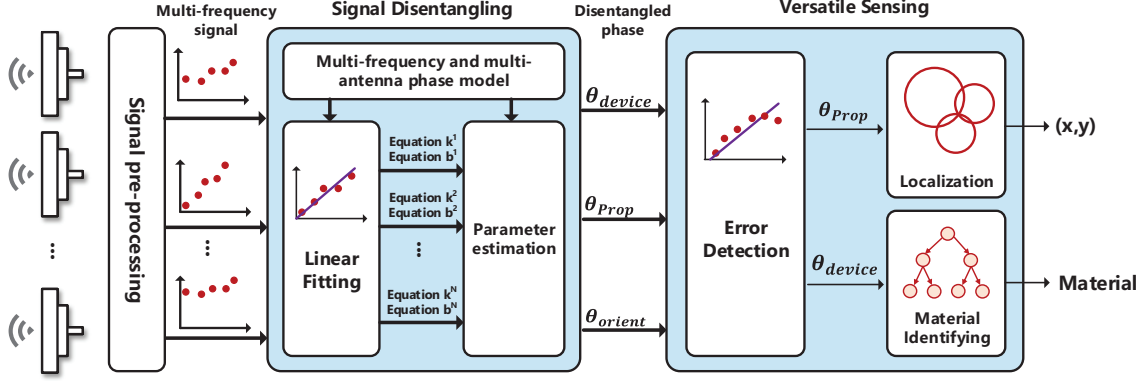


Fig. 2. System Overview of RF-Prism.

III. OVERVIEW

RF-Prism is a versatile sensing system that can simultaneously infer multiple physical states of a target (e.g., its location, orientation, and material), relying purely on the phase reading from the COTS RFID tag attached to it.

RF-Prism consists of one COTS RFID reader and several COTS tags to label the target objects. The reader is equipped with multiple circularly-polarized antennas. We use three antennas in 2D localization and four antennas for 3D localization. The antennas are placed at different locations and face toward the working region. The accurate coordinates and directions of the antennas are measured during the deployment. In the sensing process, the reader communicates with the tags across different frequency channels, during which the tags response to the reader and the phase change under different frequencies can be observed and utilized for sensing.

Fig. 2 shows the system architecture of RF-Prism, which is composed of three modules:

Signal pre-processing module. This module is used to denoise the raw phase readings provided by the commodity RFID reader, deal with the 2π folding problem, and correct the sudden π jump for latter processing.

Signal disentangling module. Based on a multi-frequency and multi-antenna phase model, this module disentangles the phase changes that caused by different factors, namely propagation distance, tag orientation, and target material, respectively. The disentangled phase signals are then feed to the sensing module for further processing.

Versatile Sensing. This module utilizes the disentangled phase signals for simultaneously localization and material sensing. To further suppress the effect of tag mobility and multi-path phenomenon, an error detector is further proposed to detect and filter out the sensing result with large errors.

The next two sections elaborate on the signal disentangling module and the versatile sensing module, providing the technical details.

IV. SIGNAL DISENTANGLING

As we have mentioned previously, the phase value of the received signal is jointly determined by multiple factors, such as the tag's location, orientation, the material of the object that the tag is attached to, and etc. As a result, to infer any one of these physical factors, a necessary assumption is that all the other factors are known and constant during the sensing process, so that all the change in phase value can be attributed to the desired factor. Such assumption is however unlikely in most sensing applications where all the physical factors are unknown and multiple factors will change simultaneously. In this case, none of the factor can be successfully inferred from the phase value.

To address the above phase entanglement problem, we in this section start with a comprehensive modeling of how different physical factors affect the received phase. We then show how to disentangle the effect of different factors by leveraging multiple carrier frequencies and multiple antennas.

A. Understanding The Phase Change In RFID Systems

In RFID communication, the reader transmits a constant single-tone carrier wave (CW) and then the tag will backscatter this CW to the reader after modulating its ID information on it. When the backscattered signal is received, the reader reports the phase reading by calculating the phase difference between the transmitted and received signals. According to [24], the phase reading θ contains four parts:

$$\theta = (\theta_{prop} + \theta_{orient} + \theta_{reader} + \theta_{tag}) \bmod 2\pi \quad (1)$$

where $\theta_{prop} = 2\pi \times \frac{2d}{\lambda}$ is the phase change caused by signal's round-trip propagation along the *antenna-tag distance* d and λ refers to the wave length of the CW signal. θ_{orient} refers to the phase rotation caused by the tag's *orientation*. θ_{reader} is related to the reader's *transmitting and receiving circuits*. θ_{tag} is determined by the tag's reflection characteristic and is relevant to the tag antenna's *impedance* [28] [31].

Equation (1) reveals two problems endemic to phased-based RFID sensing:

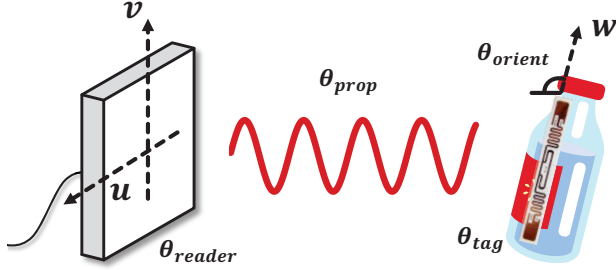


Fig. 3. Different phase components of RFID signal.

- *The phase entanglement problem:* it is infeasible to infer any of the four unknown physical factor using only one equation.
- *The phase ambiguity problem:* phase wraps around every wavelength, so when trying to infer the antenna-tag distance d , we can only recover a fractional distance modulo the wavelength. That is why phase information is typically used to infer the target's relative displacement but not exact location.

Past sensing systems address these two problems by either treating some of the physical factors as noise (thus sacrificing the sensing accuracy) or limiting their application to some particular scenarios (e.g., localizing a target with known orientation and material). Different from those works, we try to solve these problems fundamentally by directly disentangling the phase signal with the information combined from multiple frequencies and multiple antennas.

B. The Multi-frequency Phase Model

RFID readers use frequency hopping to avoid interference. A typical UHF reader hops between 50 channels in the $902\text{MHz} \sim 928\text{MHz}$ ISM band. The channel hopping capability of RFID systems provide an opportunity to combine more information for phase signal disentangling. By extending the phase model in Eq. (1) to the multi-frequency scenario, we have:

$$\theta(f) = (\theta_{prop}(f) + \theta_{orient}(f) + \theta_{reader}(f) + \theta_{tag}(f)) \bmod 2\pi \quad (2)$$

where $f \in \{f_1, \dots, f_n\}$ ($n = 50$) is the center frequency of the CW signal.

To show how multi-frequency information helps in disentangling phase signal and solving phase ambiguity problem, we in the following discuss how each part of the phase reading changes with frequency.

Propagation-dependent phase. The relationship between the propagation-dependent phase θ_{prop} and the frequency f has been widely explored in existing works [32], which is given by:

$$\theta_{prop}(f) = (2\pi \times \frac{2df}{c}) \bmod 2\pi \quad (3)$$

where c is the speed of EM waves. Eq. (3) tells that with a certain distance d , θ_{prop} changes linearly with the frequency

f . The slop of the line gives the distance d . In this way, the phase ambiguity problem is solved since d is inferred based on the changing rate of the phase (i.e., the slop), but not the exact phase value. As a verification, Figure 4 shows the phase reading θ collected under different frequency when the antenna-tag distance d is set at 0.5m, 1.5m, and 2.5m, while other factors remain constant. We can see a clear linear relationship between θ and the frequency f . Further, the slopes of different d are distinct.

Orientation-dependent phase. According to [24], when a signal propagates from a circularly-polarized antenna to a linearly-polarized tag, the tag's polarized vector w will affect the phase value θ_{orient} as:

$$\tan(\theta_{orient}) = \frac{2(u \cdot w)(v \cdot w)}{(u \cdot w)^2 - (v \cdot w)^2} \quad (4)$$

where u and v are the horizontal and vertical unit directional vectors of the reader's antenna, as illustrated in Figure 3. The direction of vector w gives the orientation of the tag. Eq (4) reveals that θ_{orient} relies only on the directions of the antenna and the tag. Frequency change have no effect on θ_{orient} because none of the variables in Eq (4) depends on the frequency of the channel. As a verification, Figure 5 shows the phase reading collected when the orientation of the tag is set at 0° , 30° , and 45° , while other factors remain constant. We can see that since θ_{orient} will not change with frequency, the change in θ_{orient} incurs the same phase shifts across all frequencies. The slopes of the line that obtained at different tag orientation are identical.

Reader and tag-dependent phase. As we have shown in Eq (1), the phase reading θ is also affected by the phase offset introduced by the imperfect hardware of the tag (denoted as θ_{tag}) and the reader (denoted as θ_{reader}). Here, θ_{tag} and θ_{reader} are typically abstracted to one parameter θ_{device} . According to [12], when a tag is attached to targets with different material, its antenna impedance will change. This impedance change will cause change in θ_{device} accordingly. Different material introduce different amount of phase change. This is why many existing works perform material identification based on θ_{device} .

To further explore the relationship between θ_{device} and f , we collect phase readings from the same tag when it is attached to targets with different materials (e.g., wood, glass, and plastic). All the other set-ups are identical across the three cases. Figure 6 shows the results. We can see that the slopes of different materials are distinct, indicating that θ_{device} changes linearly with the frequency as:

$$\theta_{device}(f) = (k_t \cdot f + b_t) \bmod 2\pi \quad (5)$$

k_t and b_t are the slop and the intercept of the line, which changes with different material. In other words, k_t and b_t contains information about the target material, thus they can be used to infer the material that a tag attached to.

Putting things together. Now, we understand how each part of the phase reading changes with frequency, as shown by Eq

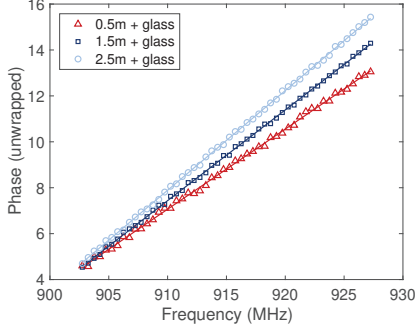


Fig. 4. θ_{prop} v.s. f .

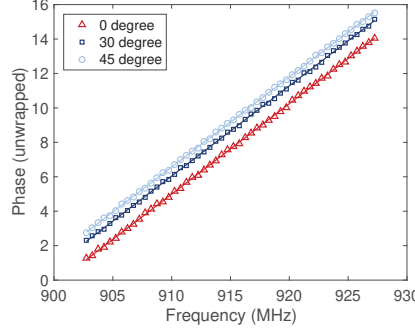


Fig. 5. θ_{orient} v.s. f .

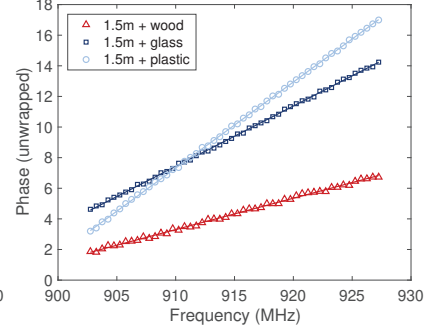


Fig. 6. θ_{device} v.s. f .

(3)~Eq (5). Substituting those equations into Eq (2), we can get the multi-frequency phase model as follows:

$$\begin{cases} \theta(f) = (k \cdot f + b) \bmod 2\pi \\ k = \frac{4\pi d}{c} + k_t \\ b = \theta_{orient} + b_t \end{cases} \quad (6)$$

Equation (6) indicates that the phase reading θ changes linearly with the frequency f . The slope of the line (i.e., k) is jointly determined by the antenna-tag distance and the target material, and the intercept of the line (i.e., b) is jointly determined by the tag orientation and the target material. By performing linear fitting on the phase reading θ collected under different frequency f , we can get b and k . That is to say, we now have two equations and four unknown parameters, i.e., d , θ_{orient} , b_t , and k_t . Although the number of equations has increased by introducing the frequency domain information, it is still difficult to disentangle each part of the phase reading from θ . We solve this problem by employing multiple reader antennas.

C. The Multi-antenna Phase Model

A localization system typically involves at least three antennas to perform triangulation. This provides us with an opportunity to further disentangle different factors in Eq (6) by adding additional equations from additional antennas. However, adding new antennas also introduce new unknown variables (i.e., new antenna-tag distance d and new tag orientation) because a new antenna will have a new coordinate and a new directional vector. That is to say, in a N -antenna system, we will have $2N$ equations and $2N + 2$ unknown variables.

Fortunately, those $2N + 2$ unknown variables are not independent. Taking the 2D localization as an example, we can express the position of the tag with a 2D coordinates (x, y) and the directional vector of the tag as (α) (in polar coordinates). Then k and b in Eq (6) can be rewritten by replacing variables d and θ_{orient} with $dist(coordinate(A^i), (x, y))$ and $\theta_{orient}(direction(A^i), \alpha)$:

$$\begin{cases} k^i = \frac{4\pi \times dist(coordinate(A^i), (x, y))}{c} + k_t \\ b^i = \theta_{orient}(direction(A^i), \alpha) + b_t \end{cases} \quad (7)$$

where $dist()$ is the Euclidean distance function. A^i refers to the i_{th} antenna, whose coordinate and direction is measured during deployment. Now we can see that *no matter how many antennas we include, the number of unknown parameters is always 5 in a 2D localization case*. Three antennas at different positions can provide enough independent equations for solving those unknown variables and getting a unique solution. When extending the problem into the 3D case, the number of unknowns will increase to 7 and four antennas are sufficient in this case. Three or four antennas are usually employed in previous multiple-antenna based RFID localization systems and the widely used Impinj R420 reader naturally support 4 different antenna ports, hence our design does not bring extra overhead.

Another problem is that when we add new antennas to the reader, we are supposed to consider the phase change caused by the antenna hardware errors. More specifically, different antennas will have different impacts on the received phase readings, resulting in different $\theta_{reader}(A^i)$ and also $\theta_{device}(A^i)$ when we query the phase values through the three (or four) antennas, although they are connected to the same reader. However, since $\theta_{reader}(A^i)$ and $\theta_{device}(A^i)$ only rely on the hardware devices, unrelated to surrounding environments, they are determined once the reader and antennas are chosen and will never be changed. Thus, we can simply correct the phase errors by switching among the different antennas for phase readings before the deployment while keeping other conditions the same, and then calculating and eliminating their differences. In this way, all antennas will have an identical θ_{reader} so that aforementioned inference still holds.

V. VERSATILE SENSING

With the phase disentangling module described in Section IV, we can separate the effect of each physical factor from the observed phase reading. The obtained parameters, *each of which is solely determined by one physical factor*, can be further employed to perform *simultaneous* and *unambiguous* estimation of all the physical factors. In this work, we take two typical application of RFID sensing (i.e., localization and material identification) as examples to demonstrate the capability of RF-Prism. We believe that with the multi-frequency multi-

antenna phase model and the idea of phase disentangling, RF-Prism can support more powerful and fancy applications.

A. Localization

As we have discussed in Section IV, the tag's coordinate (x, y) and its orientation α can be directly obtained by solving the $2N$ functions provided by the N antennas. Compared with the existing RFID-based localization, the localization method in RF-Prism provides the following advantages:

- Tag's coordinate is directly extracted from the phase term that solely related to signal propagation (i.e., θ_{prop}). As a result, RF-Prism does not rely on a calibration process to estimate and compensate for the phase offset that caused by hardware diversity of the reader-tag pair and the material of the target that the attached to (i.e., θ_{device}).
- Since a tag's coordinate and orientation are extracted simultaneously, RF-Prism does not assume static and known tag orientation during localization.
- Based on the information from multiple frequencies, we can resolve the phase ambiguity problem without exploiting antenna arrays and AoA information.

In summary, RF-Prism is the first to achieve calibration-free localization based purely on the phase reading from COTS tags, without incurring any extra hardware overhead (e.g., the antenna array).

B. Material Identification

In the design of RF-Prism, material identification is performed based on the parameters k_t and b_t , which is proved to be highly related to the material of the target that the tag attached to. However, k_t and b_t is not solely determined by the target material, it is also related to the hardware diversity of the reader-tag pair, which is mainly caused by imperfect manufacturing. So, before using k_t and b_t for material identification, we should first compensate for this hardware diversity through a calibration process.

Calibration. Since the impact of device diversity is invariant in the whole sensing process, we can compensate for it by performing a pre-calibration before the deployment. In the calibration process, we place each tag T_i (without attaching it to any object) at a known position with known orientation and collect the phase reading across all channels. The phase reading $\theta(f)$ can be expressed as:

$$\theta(f) = (\theta_{prop}(f) + \theta_{orient}(f) + \theta_{device_0}^{(T_i)}(f)) \bmod 2\pi \quad (8)$$

where $\theta_{device_0}^{(T_i)}$ is the phase term that solely determined by the i -th reader-tag pair. By subtracting the known θ_{prop} and θ_{orient} from the above equation, we can calculate $\theta_{device_0}(f)$ and store it in a database. For identifying the material of tag T_i , we subtract $\theta_{device_0}^{(T_i)}(f)$ from the tag reading $\theta(f)$ to compensate the device diversity. Note that different from the calibration of θ_{device} which should be performed once the tag is deployed in different environment or attached on different target, the calibration of θ_{device_0} is need to performed only once for each tag. And this calibration is required only when RF-Prism is used for material identification.

Feature extension. In the existing material identification methods, complex hardware structures (tag array) or dedicate tag behavior (e.g., moved by a robot) are required to eliminate the impact of other factors, such as the reader-tag distance and the orientation of the tag. Different from those methods, we can directly extract parameters, i.e., k_t and b_t , which is solely determined by the target material (after calibration) from the phase reading. In RF-Prism, k_t and b_t are the main features that is used for material identification. To further mitigate the frequency-selective fading, we include $\theta_{material}(f) = \theta_{device}(f) - \theta_{device_0}(f)$ that collected under different f into the feature vector. So finally the feature vector that used for material identification is:

$$F = (k_t, b_t, \theta_{material}(f_1) \dots \theta_{material}(f_n)) \quad (9)$$

After extracting the features form the phase reading, RF-Prism employs a classifier to identify the target material. In Section VI, we tested performance of three commonly used classifiers: K-Nearest Neighbor(KNN), Support Vector Machine(SVM) and Decision Tree. The result show that Decision Tree provides the best classification accuracy, so we choose Decision Tree for material identification. The details about how we construct the training dataset and the performance of the three classifiers are introduced in Section. VI.

C. Error Detector

One assumption underlying RF-Prism is that the physical state of the tag and the target material remain static during the time when the reader hopping across the whole frequency band. Tag's movement or rotating within this period will incurs high localization and sensing error. To solve this problem, an error detector is designed to find and filter out the time windows which contain data that collected when the tag is moving or rotating.

The basic insight is that when the tag is static, the phase readings will change linearly with the frequency, according to our empirical study in Section IV. However, if the tag is moving or rotating during the frequency hopping process, the collected phase reading under different frequency are indeed correspond to different antenna-tag distances and tag orientations. In this case, the linear relationship will not hold any more. Thus, we can detect the movement and rotation of the tag by simply checking whether a linearity relationship still holds between the phase reading and the frequency.

D. Multipath Suppression

The linear relationship check is also helpful for suppressing the multipath effect which is also a common problem in RFID sensing systems. According to [13], [20], an important observation is that the phase readings change linearly over the carrier frequencies if the multipath effect is negligible (or in other words the LOS signals dominates). Otherwise, in a multipath environment, the phase readings at different channels suffer from different superposition of phase from all propagation paths. This can also result in nonlinear changes of the phase readings. Different from the mobility case, if there

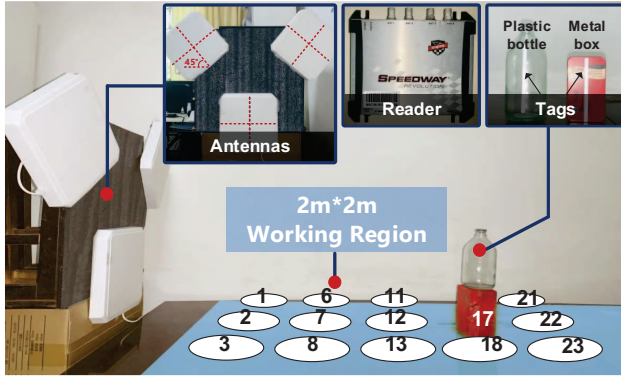


Fig. 7. Experimental setup of RF-Prism.

still exists a relatively stronger direct-path signal, multipath effects will not totally break the linear relationship like what happens when the tag is moving, but make the samples on some frequencies largely deviate while the remaining samples can still be fitted into a line.

So in this case, we can just identify the outliers on those frequencies which are affected a lot by multipath and pick up the relatively "clean" channels for localization and sensing. Commercial RFID readers hopping their channels over 50 different frequencies within $902 \sim 928 MHz$. It is more than enough for a linear fitting so this selection can be conducted.

VI. EVALUATION

A. Implementation

We implement a prototype of RF-Prism using a commodity Impinj Speedway R420 RFID reader, three Laird S9028PCL circularly-polarized antennas, and Alien EPC Gen2 UHF passive RFID tags. The reader works at the UHF frequency band $902.75 - 927.25 MHz$ and hops over 50 frequency channels. The reader costs about \$1500 and 3 antennas costs about \$400.

For back-end software, we use the Impinj Octane SDK Toolkit to connect and control the reader for data collection via an Ethernet cable. Data processing and localization/material identification algorithms are developed in MATLAB. All the software components run at a PC, which is equipped with Intel Core i5-8600 CPU and 16G memory.

B. Methodology

The experiment setup is shown in Fig. 7. The three antennas are placed with $0.5m$ spacing to each other, facing with a $2m \times 2m$ working region. The coordinates and directions of the antennas are measured before experiments.

For localization, the tags are placed at 25 points with known positions as ground truth. To further test RF-Prism's performance in orientation sensing, we rotate the tags by 0° , 30° , 60° , 90° , 120° , and 150° respectively at each position. We repeat the measurement for every rotation degree 5 times so the experiments are repeated 30 times at each position. During the experiment, the tag is attached to a plastic object which do not affect the tag's signal feature.

For material identification, 8 different types of material are tested, including 4 solid objects (wood, plastic, glass, metal) and 4 liquids (water, skim milk, edible oil, 75% medical alcohol). All these materials are easy to fetch in daily lives. We choose those material types according to their different conductivity, so we can detect the phase differences caused by them and then identify them. If two kinds of materials have similar conductive characteristics (like 50% and 60% alcohol), the sensing system hardly can differentiate between them. Note that the RFID tag often stops working when its circuits are directly attached to a metal surface, hence we place two pieces of paper between the tag and the metal surface to ensure we can collect the data successfully. When performing liquid identification, the liquid are contained in an identical glass bottle. For each type of material, measurements are repeated 150 times (100 for 0° and 50 for 90°) at different positions in the working region. 50% of the trials in 0° are used as training set and the others are used for validation. We evaluate the material identification performance in terms of the accuracy for a 8-class classification problem.

Comparison: We compare RF-Prism with two state-of-the-art approaches:

- **Mobitagbot** uses two antennas and also leverages the multi-channel technique to improve the localization. But Mobitagbot cannot eliminate the effect of orientation, device, and material related phase offset.
- **Tagtag** performs material identification based on the DTW algorithm. It eliminates the impact of signal propagation using the the RSS readings.

C. Overall Performance

In this section, we test the performance of RF-Prism on localization, orientation sensing, and material identification.

Location Errors. The localization performance of RF-Prism is evaluated under varying orientations and materials. The result is shown in Fig. 8. RF-Prism achieve a mean location error of $7.61cm$ across the degrees from 0° to 150° . Different degrees show similar results and the maximum different (between 30° and 150°) is only $0.70cm$. This verifies RF-Prism's ability in phase disentangling which enables it to eliminate the effect from orientation on localization. When changing the material of the target object, we fix the tag's orientation at 0° . RF-Prism achieve a mean location error of $7.48cm$ across 8 materials. Among the four solid materials, the location error of metal is slightly higher than that of other three materials, probably because that metal surfaces will cause a strong signal reflection which buries the signal backscattered from tags (which we use for sensing). Due to the similar reason, the non-conductive oil performs better than other conductive liquids.

Orientation Errors. Figure 9 shows the orientation errors of RF-Prism when the tag is located at different positions and attached to targets with different materials. We divide all the positions into three different regions, i.e., near, medium and far, based on the tag-antenna distances. The results in the near, medium and far regions are 8.59° , 10.40° and 10.50° ,

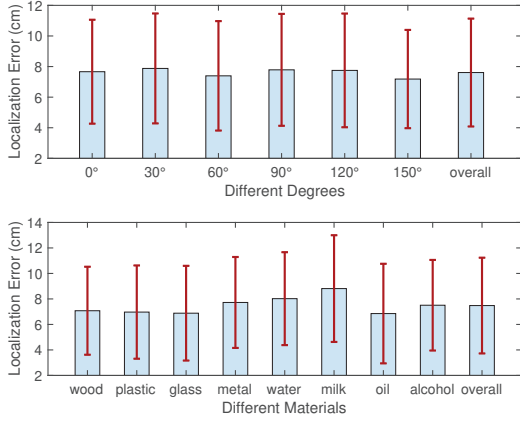


Fig. 8. Overall location errors with different orientations and materials.

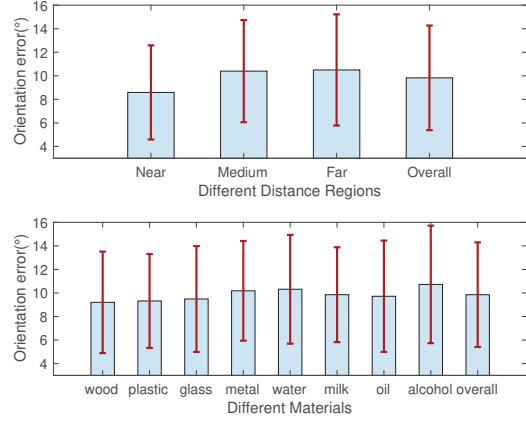


Fig. 9. Overall orientation errors with different locations and materials.

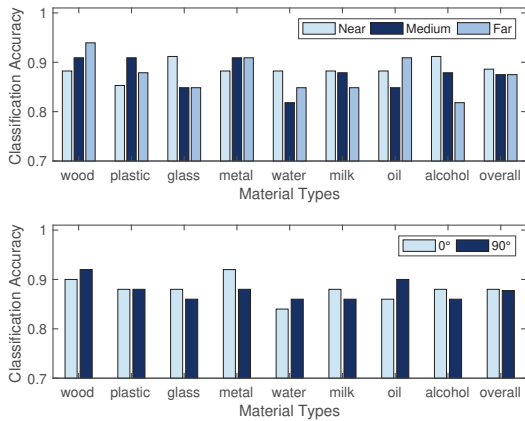


Fig. 10. Overall material identification accuracy with different locations and materials.

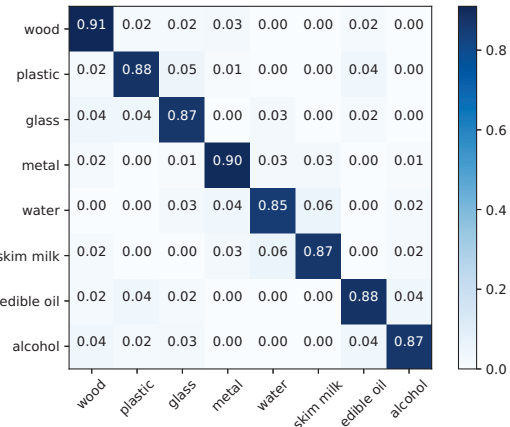


Fig. 11. Confusion matrix of all 8 material types.

respectively. RF-Prism achieves higher orientation accuracy in near regions than in medium and far regions. We think the reason behind is that when the antenna and the tag are close, line-of-sight signals are stronger and impacted less by other unexpected signals like reflected signals from the ground or white noises in the environment. We find that metal and the three conductive liquids have a slightly higher errors than others due to similar reasons in the analysis of location errors.

Material Identification Accuracy. Fig. 10 shows the material identification accuracy of RF-Prism with different positions and orientations. Positions are also divided into near, medium, and far regions, and the corresponding material identification accuracy are 88.6%, 87.5% and 87.5%, respectively. In average, the result in near region is also slightly better than those in medium and far regions, but this observation is inconsistent for different material types. We also test the performance of material identification in two different tag orientations: 0° and 90° . The results show that, with only the

training data at 0° , RF-Prism still achieves ideal and similar performance (88.0% and 87.8%) at 0° and 90° . Consequently, we believe that different distances or orientations do not have significant impacts on material identification in RF-Prism.

Figure 11 further shows the confusion matrix of the material identification result. For almost all the materials, the classification accuracy is higher than 87%, except water (85%). The result tells that water is easy to be confused with skim milk (6%), probably because water and skim milk have similar conductive characteristics such as permittivity. Unlike the results in the localization and orientation sensing experiments, metal gets a high accuracy in material identification (90%). That is because that the performance of material identification relates not only to the performance of phase disentangling, but also the natural feature discrimination between different materials. Although metal produces stronger interference, it exhibits more distinguishable features compared with other materials.

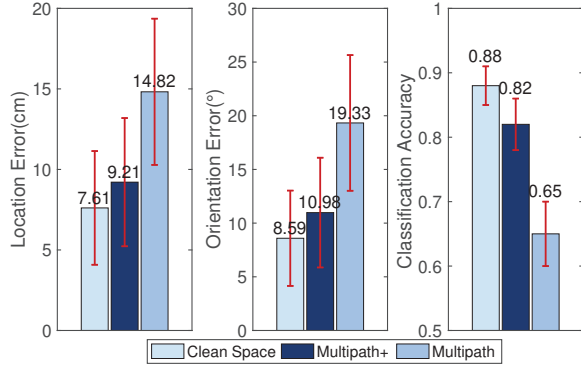


Fig. 12. System performance in different environments.

Impacts of multipath effect. In order to evaluate the impact of multipath interference on RF-Prism and the performance of the multipath suppression method described in Section V-D, we conduct experiments under two different scenarios: (1) a clean space without any other surrounding objects; (2) a multipath setup with some cartons and people around the RFID tag and the antennas, but the LOS propagation is still guaranteed. The results in terms of the localization error, orientation error, and material classification accuracy are shown in Figure 12. The "Multipath+" bar and "Multipath" bar stand for RF-Prism system with and without the multipath suppression method. We can find that multipath effect can actually cause a significant performance degradation. Without the multipath suppression method, the localization error and orientation error in a multipath environment are roughly $2\times$ than those in a clean space, and the material classification accuracy suffers a drop of 23%. The main reason behind is that the multipath signals can interfere with the LOS signal, resulting in inaccurate results when we calculate the phase parameters. Another important observation is that our channel selection method can effectively suppress the multipath effect and achieves similar performance with the result obtained in clean space. It produces 37.8%, 43.2%, and 26.1% performance gain in localization, orientation estimation, and material classification, respectively.

Noises caused by the signal interference from other RF devices in the environment can also impact greatly the system performance since phase measurements may be inaccurate or even inaccessible. But different from the multipath effect, noises are usually transient so RF-Prism is more likely to filter out them just like in the mobility error case.

Performance of different classifiers. We also test the performance of three widely used classifiers for material classification: K-Nearest Neighbor (KNN), Support Vector Machine (SVM) and Decision Tree. The results is shown in Fig. 13. The accuracy of KNN, SVM and Decision Tree are 75.6%, 83.5%, and 87.9% respectively. Clearly, Decision Tree outperforms the other two classifiers. The possible reason behind is that: 1) KNN dose not work well with high dimensional data while the dimension of the feature vector we defined is 52. 2) The

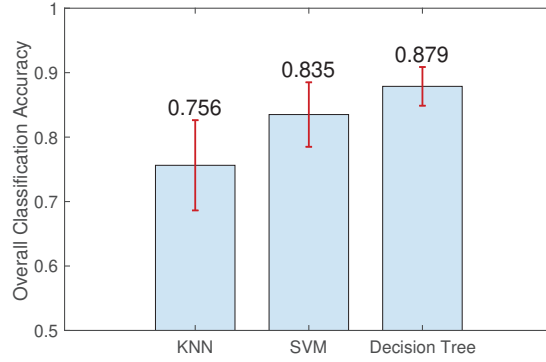


Fig. 13. Material identification accuracy with different classifiers.

performance of SVM varies with different kernel functions, but usually it is not easy to find the optimal kernel function.

Latency of Sensing. The time overhead of RF-Prism mainly lies on three components: i) data gathering with channel hopping, ii) data pre-processing and parameter estimation with linear fitting, iii) sensing. In our implementation, data pre-processing and parameter estimation can be completed within 0.06s. The localization results are obtained once the parameter estimation is done. The time overhead for the three classifiers are all within dozens of milliseconds. The data gathering component dominates the overall time overhead. For example, the ImpinJ R420 reader we use has to spend 200ms on each channel, so a hopping round covering all the 50 channels will cost 10s. This problem is totally caused by the hardware limitation. On other platforms which can complete the channel hopping within shorter periods or allow users to customize the hopping pattern, RF-Prism can also work in a much faster way.

D. Case Study 1: Localization

The key advantage of RF-Prism is it can simultaneously extract multiple factors from the phase reading, thus its performance in localization will not be affected by the tag's orientation and the material of the target. To see how this ability benefits the existing RFID-based localization technologies, we compare RF-Prism with Mobitagbot, a localization method which cannot mitigate the impact of tag orientation or target material on the localization process. Fig. 14 shows the CDF (Cumulative Distribution Function) of the localization error when the orientation of the tag is invariant (at 0 degree) and the object attached to the tag is unchanged. As we can see, RF-Prism achieves a mean location error of 7.33cm and a maximum error of 16cm. MobiTagbot gets a little bit higher but very similar mean location error of 8.25cm. It implies RF-Prism and MobiTagbot exhibit the same level performance in localization if there is no interference from other factors. Then we rotate the tag and further change the material of the object to see how the varying orientation and material affect the localization performance of these two systems. The results are shown in Fig. 15 and Fig. 16. We can see that the performance of MobiTagbot degrade

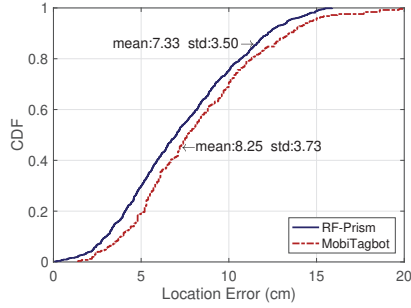


Fig. 14. Localization error CDF with the same orientation and material.

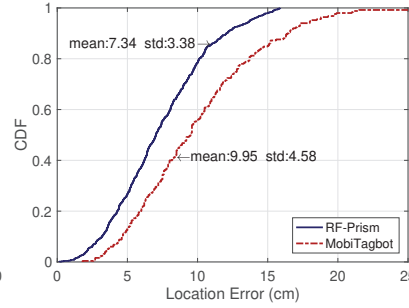


Fig. 15. Localization error CDF with the same material but different orientations.

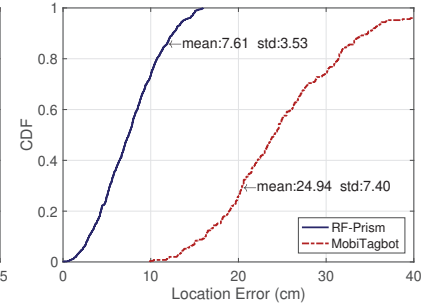


Fig. 16. Localization error CDF with different orientations and materials.

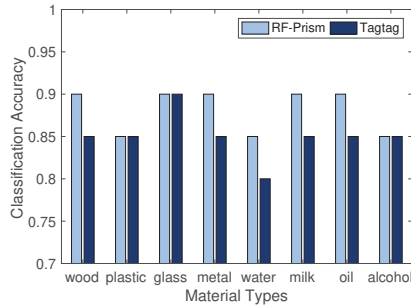


Fig. 17. Material identification accuracy with the same distance and orientation.

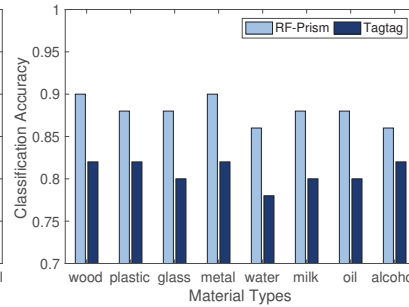


Fig. 18. Material identification accuracy with the same orientation but different distances.

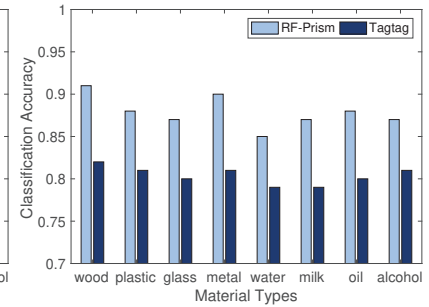


Fig. 19. Material identification accuracy with different distances and orientations.

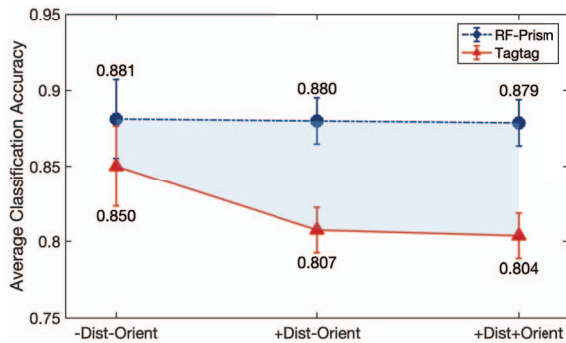


Fig. 20. Overall average classification accuracy of RF-Prism and Tagtag with different setups.

significantly with more varying factors: with a changing orientation, the performance of MobiTagbot degrades by about 20%, then the changing material further introduces another 150% performance degradation. In contrast, RF-Prism always exhibit ideal and consistent localization accuracy even under varying orientation and material. It exhibits more apparent performance gain with more varying factors, which should be attributed to RF-Prism's ability to extract the phase term that solely related to the propagation distance. In contrast, Mobitagbot only considers the orientation/material-dependent and phase change as random noises, thus resulting in relatively poor performance.

E. Case Study 2: Material Identification

Similarly, the performance of RF-Prism in material identification is also immune to factors like signal propagation distances or tag orientations. To further show how this ability benefit the existing material identification methods, we compare RF-Prism with Tagtag. Fig. 17 ~ 19 compares the identification performance of RF-Prism and Tagtag under setups with different number of varying factors. RF-Prism consistently outperforms Tagtag and the performance gain becomes more apparently with more varying factors.

Fig. 20 summarizes the overall material identification accuracy of RF-Prism and Tagtag under those three different setups. The minus symbol in the x label means the corresponding factor is kept unchanged in the experiment while the plus symbol means it is a variant factor. We can see that when both the tag-antenna distance and the tag's orientation are invariant, RF-Prism and Tagtag achieve similar mean identification accuracy (88.1% and 85.0%, respectively). However, when we place the target at different positions, the identification accuracy of RF-Prism is still 88.0% while that of Tagtag degrades to 80.7%. The reason behind is that Tagtag eliminates the impact of the antenna-tag distance by simply leveraging the coarse RSS readings. We also find that rotating the tag does not further enlarge the performance gap. This is because that Tagtag also uses channel hopping to cancel the impact of tag orientations.

Note that although Tagtag shows similar performance with RF-Prism in some cases, there is still a fundamental differ-

ence between these two methods. Specifically, Tagtag tries to mitigate the impact of all the other physical factors while RF-Prism is essentially designed for phase disentangling, which fundamentally addresses the phase entanglement problem. Thus it can be used in many other sensing applications, and do not stop at the two examples shown in this paper.

VII. DISCUSSION & CONCLUSION

In this work, we propose RF-Prism, a versatile RFID sensing system that can simultaneously infer multiple physical factors from one phase readings. Based on a comprehensive understanding of how different factors affect the phase reading, we design a phase disentangling method to extract the phase change attributed to different factors. The disentangled phase signals are further utilized to simultaneously infer the location, the orientation, and the material of the target. We implement the prototype of RF-Prism with COTS RFID devices and conduct extensive experiments to evaluate the performance of RF-Prism. Experimental results verifies RF-Prism's ability in simultaneously estimating multiple physical factors and show that for any of the three factors, RF-Prism always outperforms the corresponding state-of-the-art sensing system.

There are some more extensions for RF-Prism that can be developed in the future work. One of them is to perform the system in 3D space, which is totally feasible as long as increasing the number of antenna to 4. Another is to apply more powerful deep-learning methods to improve the performance of material identification. It dose not conflict with the existing system, too. The reason why only basic methods are tested in this paper is that we want to avoid confusing the performance gain caused by phase disentangling and advanced classification methods such as neural networks.

VIII. ACKNOWLEDGMENTS

We sincerely thank our shepherd and the reviewers for their valuable feedback. This work is supported in part by National Key R&D Program of China No. 2017YFB1003000 and the R&D Project of Key Core Technology and Generic Technology in Shanxi Province (2020XXX007).

REFERENCES

- [1] L. Xie, C. Wang, Y. Bu, J. Sun, Q. Cai, J. Wu, and S. Lu, "Taggedar: An rfid-based approach for recognition of multiple tagged objects in augmented reality systems," *IEEE Transactions on Mobile Computing*, vol. 18, no. 5, pp. 1188–1202, 2018.
- [2] C. Zhao, Z. Li, T. Liu, H. Ding, J. Han, W. Xi, and R. Gui, "Rf-mehndi: a fingertip profiled rf identifier," in *Proceedings of IEEE INFOCOM*, 2019.
- [3] J. C. Chen, C.-H. Cheng, P. B. Huang, K.-J. Wang, C.-J. Huang, and T.-C. Ting, "Warehouse management with lean and rfid application: a case study," *The International Journal of Advanced Manufacturing Technology*, vol. 69, no. 1–4, pp. 531–542, 2013.
- [4] F. Tian, "An agri-food supply chain traceability system for china based on rfid & blockchain technology," in *Proceedings of IEEE ICSSM*, 2016.
- [5] A. Ali and M. Haseeb, "Radio frequency identification (rfid) technology as a strategic tool towards higher performance of supply chain operations in textile and apparel industry of malaysia," *Uncertain Supply Chain Management*, vol. 7, no. 2, pp. 215–226, 2019.
- [6] R. Y. Zhong, S. Lan, C. Xu, Q. Dai, and G. Q. Huang, "Visualization of rfid-enabled shopfloor logistics big data in cloud manufacturing," *The International Journal of Advanced Manufacturing Technology*, vol. 84, no. 1–4, pp. 5–16, 2016.
- [7] L. Yang, Y. Chen, X.-Y. Li, C. Xiao, M. Li, and Y. Liu, "Tagoram: Real-time tracking of mobile rfid tags to high precision using cots devices," in *Proceedings of ACM Mobicom*, 2014.
- [8] Z. Luo, Q. Zhang, Y. Ma, M. Singh, and F. Adib, "3d backscatter localization for fine-grained robotics," in *Proceedings of USENIX NSDI*, 2019.
- [9] C. Wang, J. Liu, Y. Chen, H. Liu, L. Xie, W. Wang, B. He, and S. Lu, "Multi-touch in the air: Device-free finger tracking and gesture recognition via cots rfid," in *Proceedings of IEEE INFOCOM*, 2018.
- [10] L. Shangguan, Z. Zhou, and K. Jamieson, "Enabling gesture-based interactions with objects," in *Proceedings of ACM MobiSys*, 2017.
- [11] H. Ding, J. Han, L. Shangguan, W. Xi, Z. Jiang, Z. Yang, Z. Zhou, P. Yang, and J. Zhao, "A platform for free-weight exercise monitoring with passive tags," *IEEE Transactions on Mobile Computing*, vol. 16, no. 12, pp. 3279–3293, 2017.
- [12] B. Xie, J. Xiong, X. Chen, E. Chai, L. Li, Z. Tang, and D. Fang, "Tagtag: material sensing with commodity rfid," in *Proceedings of ACM Sensys*, 2019.
- [13] J. Wang, J. Xiong, X. Chen, H. Jiang, R. K. Balan, and D. Fang, "Tagscan: Simultaneous target imaging and material identification with commodity rfid devices," in *Proceedings of ACM MobiCom*, 2017.
- [14] Z. Chen, P. Yang, J. Xiong, Y. Feng, and X.-Y. Li, "Tagray: Contactless sensing and tracking of mobile objects using cots rfid devices," in *Proceedings of IEEE INFOCOM*, 2020.
- [15] Y. Zheng, Y. He, M. Jin, X. Zheng, and Y. Liu, "Red: Rfid-based eccentricity detection for high-speed rotating machinery," in *Proceedings of IEEE INFOCOM*, 2018.
- [16] P. Li, Z. An, L. Yang, and P. Yang, "Towards physical-layer vibration sensing with rfids," in *Proceedings of IEEE INFOCOM*, 2019.
- [17] Y. Ma, N. Selby, and F. Adib, "Minding the billions: Ultra-wideband localization for deployed rfid tags," in *Proceedings of ACM MobiCom*, 2017.
- [18] T. Liu, Y. Liu, L. Yang, Y. Guo, and C. Wang, "Backpos: High accuracy backscatter positioning system," *IEEE Transactions on Mobile Computing*, vol. 15, no. 3, pp. 586–598, 2015.
- [19] H. Xu, D. Wang, R. Zhao, and Q. Zhang, "Faho: deep learning enhanced holographic localization for rfid tags," in *Proceedings of ACM SenSys*, 2019.
- [20] L. Shangguan and K. Jamieson, "The design and implementation of a mobile rfid tag sorting robot," in *Proceedings of ACM Mobisys*, 2016.
- [21] J. Wang and D. Katabi, "Dude, where's my card? rfid positioning that works with multipath and non-line of sight," in *Proceedings of ACM SIGCOMM*, 2013.
- [22] T. Wei and X. Zhang, "Gyro in the air: tracking 3d orientation of batteryless internet-of-things," in *Proceedings of ACM MobiCom*, 2016.
- [23] C. Jiang, Y. He, X. Zheng, and Y. Liu, "Orientation-aware rfid tracking with centimeter-level accuracy," in *Proceedings of ACM/IEEE IPSN*, 2018.
- [24] C. Jiang, Y. He, S. Yang, J. Guo, and Y. Liu, "3d-omnitrack: 3d tracking with cots rfid systems," in *Proceedings of ACM/IEEE IPSN*, 2019.
- [25] S. Manzari, C. Occhiuzzi, S. Nawale, A. Catini, C. Di Natale, and G. Marrocco, "Humidity sensing by polymer-loaded uhf rfid antennas," *IEEE Sensors Journal*, vol. 12, no. 9, pp. 2851–2858, 2012.
- [26] A. Vena, E. Perret, D. Kaddour, and T. Baron, "Toward a reliable chipless rfid humidity sensor tag based on silicon nanowires," *IEEE Transactions on Microwave Theory and Techniques*, vol. 64, no. 9, pp. 2977–2985, 2016.
- [27] L. Yang, Y. Li, Q. Lin, H. Jia, X.-Y. Li, and Y. Liu, "Tagbeat: Sensing mechanical vibration period with cots rfid systems," *IEEE/ACM transactions on networking*, vol. 25, no. 6, pp. 3823–3835, 2017.
- [28] S. Pradhan, E. Chai, K. Sundaresan, L. Qiu, M. A. Khojastepour, and S. Rangarajan, "Rio: A pervasive rfid-based touch gesture interface," in *Proceedings of ACM MobiCom*, 2017.
- [29] J. Guo, T. Wang, Y. He, M. Jin, C. Jiang, and Y. Liu, "Twinleak: Rfid-based liquid leakage detection in industrial environments," in *Proceedings of IEEE INFOCOM*, 2019.
- [30] J. Guo, T. Wang, M. Jin, S. Yang, C. Jiang, L. Liu, and Y. He, "Tagleak: Non-intrusive and battery-free liquid leakage detection with backscattered signals," in *Proceedings of IEEE ICI*, 2018.
- [31] M. D. Daniel *et al.*, "The rf in rfid passive uhf rfid in practice," *Elsevier*, 2008.
- [32] X. Li, Y. Zhang, and M. G. Amin, "Multifrequency-based range estimation of rfid tags," in *Proceedings of IEEE RFID*, 2009.